

UC Santa Barbara

UC Santa Barbara Previously Published Works

Title

Cross-plane lattice and electronic thermal conductivities of ErAs : InGaAs/InGaAlAs superlattices

Permalink

<https://escholarship.org/uc/item/1f8240bn>

Journal

Applied Physics Letters, 88(24)

ISSN

0003-6951

Authors

Kim, W

Singer, S L

Majumdar, A

et al.

Publication Date

2006-06-01

Peer reviewed

Cross-plane lattice and electronic thermal conductivities of ErAs:InGaAs/InGaAlAs superlattices

Woochul Kim, Suzanne L. Singer, and Arun Majumdar^{a)}

Department of Mechanical Engineering, University of California, Berkeley, California 94720

Daryoosh Vashaee, Zhixi Bian, and Ali Shakouri

Department of Electrical Engineering, University of California, Santa Cruz, California 95064

Gehong Zeng and John E. Bowers

Department of Electrical and Computer Engineering, University of California, Santa Barbara, California 93106

Joshua M. O. Zide and Arthur C. Gossard

Department of Materials, University of California, Santa Barbara, California 93106

(Received 21 December 2005; accepted 1 May 2006; published online 13 June 2006)

We studied the cross-plane lattice and electronic thermal conductivities of superlattices made of InGaAlAs and InGaAs films, with the latter containing embedded ErAs nanoparticles (denoted as ErAs:InGaAs). Measurements of total thermal conductivity at four doping levels and a theoretical analysis were used to estimate the cross-plane electronic thermal conductivity of the superlattices. The results show that the lattice and electronic thermal conductivities have marginal dependence on doping levels. This suggests that there is lateral conservation of electronic momentum during thermionic emission in the superlattices, which limits the fraction of available electrons for thermionic emission, thereby affecting the performance of thermoelectric devices. © 2006 American Institute of Physics. [DOI: 10.1063/1.2207829]

The performance of thermoelectric energy conversion devices depends on the thermoelectric figure of merit (ZT) of a material, which is defined as $ZT = S^2 \sigma T / k$ where S , σ , k , and T are the Seebeck coefficient, electrical conductivity, thermal conductivity and absolute temperature, respectively. As shown in the expression, low thermal conductivity and high power factor ($S^2 \sigma$) are essential for efficient operation of thermoelectric devices. Since the electronic thermal conductivity of thermoelectric materials is proportional to their electrical conductivity via the Wiedemann-Franz law, only the lattice thermal conductivity of the material should be reduced.^{1,2} Therefore, precise estimation of lattice and electronic thermal conductivities is essential in efforts to increase the ZT of the material. Recently, semiconductor superlattices have shown promises for increasing ZT for their low thermal conductivity.^{2,3} Even so, studies on the effects of electronic thermal conductivity on the total thermal conductivity of thermoelectric superlattices are scarce^{1,4,5} and somewhat preliminary. In this letter, cross-plane total thermal conductivity of the superlattices was measured at different doping levels. Theoretical analysis of cross-plane electrical conductivity of the samples was used to predict electronic thermal conductivity and to extract lattice thermal conductivity from the measurements.

Figure 1 is a schematic showing samples of one period of the superlattices. One component of the superlattices included a 10 nm thick film of $\text{In}_{0.53}\text{Ga}_{0.28}\text{Al}_{0.19}\text{As}$ (InGaAlAs). The second component was a 20 nm thick film of $\text{In}_{0.53}\text{Ga}_{0.47}\text{As}$ containing epitaxially embedded ErAs nanoparticles (denoted as ErAs:InGaAs). The ErAs concentration was 0.3% in all the samples. The samples were grown on an InP substrate with a buffer layer of 50 nm of

n -InGaAs using a molecular beam epitaxy (MBE) system. The growth temperature was 490 °C. The total thickness of the superlattice was 2.1 μm . Semimetallic ErAs nanoparticles provided $2 \times 10^{18} \text{ cm}^{-3}$ of doping,⁶ which formed the base line doping. Silicon was used as a codopant and it introduced charge carriers in the ErAs:InGaAs regions of 0, 2×10^{18} , 4×10^{18} , and $8 \times 10^{18} \text{ cm}^{-3}$, respectively. Therefore, the effective carrier concentrations in the four samples were 2×10^{18} , 4×10^{18} , 6×10^{18} , and $10 \times 10^{18} \text{ cm}^{-3}$, respectively. For the purpose of thermal conductivity measurements, a silicon dioxide layer ($\sim 0.18 \mu\text{m}$) was deposited on top of the samples. The differential 3ω method was used to measure thermal conductivity.⁷ A platinum ($\sim 380 \text{ nm}$ in thickness and $30 \mu\text{m}$ wide) film with a chromium ($\sim 4 \text{ nm}$ thick) adhesion layer was patterned on top of the silicon dioxide layer as the heater and thermometer.

The reason for choosing the combination of these materials to increase ZT is as follows. InGaAlAs is known to have a band offset of $\Delta = 0.2 \text{ eV}$ with respect to ErAs:InGaAs, which could increase the thermopower of the sample by approximately Δ/qT where q is the charge of an electron/hole. The role of ErAs:InGaAs is to reduce the thermal conductivity

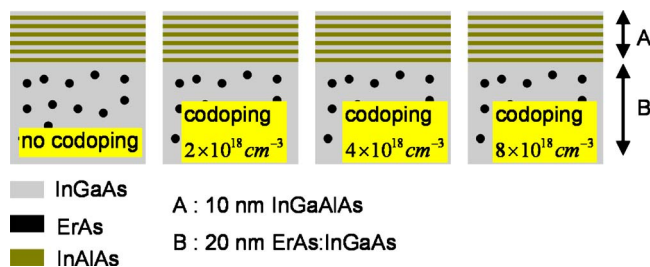


FIG. 1. (Color online) A schematic showing samples of one period of ErAs:InGaAs/InGaAlAs with different doping levels.

^{a)}Electronic mail: majumdar@me.berkeley.edu

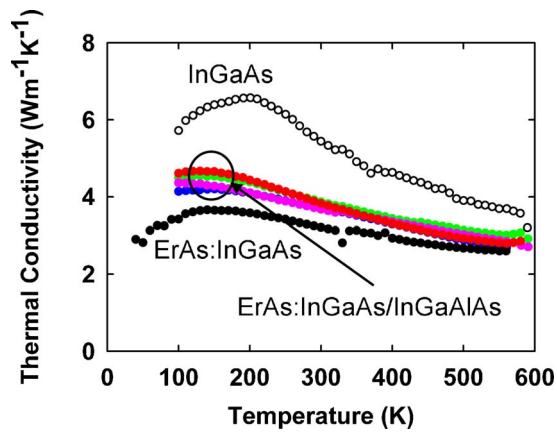


FIG. 2. (Color online) Thermal conductivity of ErAs:InGaAs/InGaAlAs superlattices with different doping levels [no codoping (red circles), codoping of $2 \times 10^{18} \text{ cm}^{-3}$ (blue circles), codoping of $4 \times 10^{18} \text{ cm}^{-3}$ (green circles), and codoping of $8 \times 10^{18} \text{ cm}^{-3}$ (pink circles)]. The thermal conductivity of InGaAs and ErAs:InGaAs is shown for reference.⁸

ity below that of InGaAs or InGaAlAs. It has been shown previously that incorporating ErAs nanoparticles 1–5 nm in diameter effectively reduces thermal conductivity below InGaAs alloy because ErAs nanoparticles effectively scatter low and midwavelength phonons while atomic substitution in InGaAs alloy scatters short wavelength phonons.⁸ The hypothesis is that a combination of high thermopower, low thermal conductivity, and possibly high electrical conductivity could increase ZT .

Figure 2 shows the cross-plane thermal conductivity of ErAs:InGaAs/InGaAlAs superlattices. The thermal conductivity of InGaAs and ErAs:InGaAs films is shown for reference.⁸ The data indicate that thermal conductivity of ErAs:InGaAs/InGaAlAs superlattices is higher than that of an ErAs:InGaAs film and yet lower than that of an InGaAs

film. However, note that doping does not produce much difference among the thermal conductivities of the superlattices even though carrier concentrations vary by a factor of 5.

Incorporating charge carriers has two effects on the thermal conductivity: (i) decrease in phonon contribution due to electron-phonon and impurity (i.e., codopant)-phonon scatterings, and (ii) increase due to electronic contribution. According to Ziman,⁹ electron-phonon scattering rate τ^{-1} depends on the electron effective mass m^* as $\tau^{-1} \sim (m^*)^3$. Therefore, considering the low effective mass of ErAs:InGaAs/InGaAlAs superlattices (about $0.043 \times m_e$ and $0.058 \times m_e$ in the well and barrier regions, respectively, where m_e is electron rest mass), electron-phonon scattering can be assumed to be negligible. In fact, a recent study⁸ on the thermal conductivity of ErAs:InGaAs film supports this hypothesis. For the impurity-phonon scattering, phonon scattering due to impurity atoms follows the Rayleigh scattering criterion,¹⁰ which suggests that high frequency phonons are scattered much more effectively than the low frequency phonons. It was speculated¹¹ that the phonon mean free path in doped GaAs might scale with the inter-codopant distance and the lattice thermal conductivity could be suppressed. In our samples, the interdopant distance in the ErAs:InGaAs layer is around 3–6 nm.¹¹ However, the interatomic distance of $\text{In}_{0.53}\text{Ga}_{0.47}\text{As}$ alloy, which also scatters high frequency phonons due to the alloy scattering, is on the order of 1 Å. Therefore, the mean free path of high frequency phonons is not affected by the impurities. Hence, the impurity-phonon scattering has negligible effect on the lattice thermal conductivity. Therefore, the lattice thermal conductivity of the four samples would be almost identical. Electronic thermal conductivity would produce the only difference between them. According to the Wiedemann-Franz law for semiconductors,¹³ the electronic thermal conductivity, k_e , can be estimated as

$$\frac{k_e}{\sigma T} = \frac{k_B^2}{q^2} \left\{ \frac{[p + (7/2)][p + (3/2)]F_{[p+(5/2)]}F_{[p+(1/2)]} - [p + (5/2)]^2 F_{[p+(3/2)]}^2}{[p + (3/2)]^2 F_{[p+(1/2)]}^2} \right\}, \quad (1)$$

where k_B is Boltzmann constant. Here, p appearing in Eq. (1) arises from the relaxation time, $\tau \approx E^p$, where E is energy of electrons. F_r is the Fermi-Dirac integral¹² of order r . However, the Wiedemann-Franz law is valid when temperature is either much lower or much higher than the Debye temperature.¹³

Figure 3 shows theoretically calculated cross-plane electrical conductivity, and cross-plane total and electronic thermal conductivities at a temperature of 580 K at various carrier concentrations. Considering the Debye temperature of InGaAs¹⁴ is 320 K, using the Wiedemann-Franz law to estimate electronic thermal conductivity at 580 K can be justified. The cross-plane electrical conductivities of the superlattices are calculated¹⁵ using a modified linear Boltzmann transport equation that takes into account the two-dimensional states in the well, i.e., ErAs:InGaAs, and three-dimensional states above the well and in the barrier region, i.e., InGaAlAs. In addition, the quantum mechanical trans-

mission coefficient that accounts for both tunneling and thermionic emission is introduced. The transmission probability was calculated using the Wentzel-Kramer-Brillouin (WKB) approximation. Finally, Fermi-Dirac statistics were used to account for the number of available empty states in the neighboring wells for tunneling and thermionic emission. Since only the wells are doped, the free carriers will transfer to the barrier regions to keep the Fermi level flat at equilibrium. This will result in the band bending and an increase of the effective barrier height, which is significant for high doping density. We consider the band bending effect in a self-consistent calculation of the effective barrier height and Fermi energy. Two cases for superlattices were studied:^{15–17} when lateral momentum during thermionic emission is conserved (C), and when lateral momentum is not conserved (NC). The lateral momentum nonconservation may happen at a rough interface, which is supposed to increase the cross-plane electrical conductivity dramatically. The actual electri-

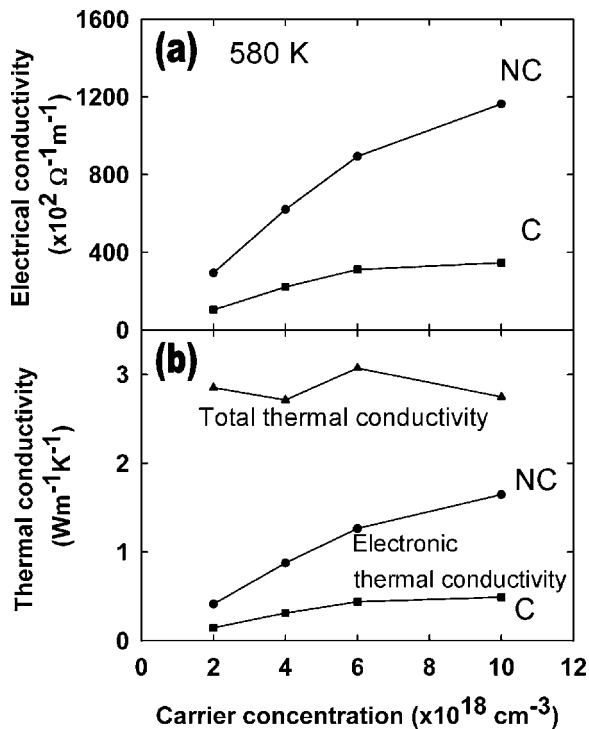


FIG. 3. (Color online) (a) Cross-plane electrical conductivity (theory); (b) cross-plane total (experimental data) and electronic thermal conductivities [based on Eq. (1)] at 580 K vs carrier concentration. In calculating the cross-plane electrical conductivity, two cases were considered: when lateral momentum during thermionic emission is conserved (C), and when lateral momentum is not conserved (NC).

cal conductivity ought to reside between these two cases. For the samples studied here, the embedded ErAs particles in the wells may introduce some non-uniformity at the InGaAs:InGaAlAs well-barrier interfaces causing non-conservation of lateral momentum in the electron transport. However, the effects of nanoparticles on the lateral momentum nonconservation require further investigation. Electronic thermal conductivity was then estimated using Eq. (1). It was assumed that electron-optical phonon scattering is the dominant scattering mechanism at 580 K, and so $p=0.5$ based on Ehrenreich's expression on the relaxation time.¹⁸ Experimental measurement uncertainty of the total thermal conductivity is around 15%–20%.

Figure 3(b) shows that the measured total thermal conductivity is almost independent of doping and has an average value of 2.8 W/m K with an uncertainty of 0.5 W/m K. This contains contribution from both the lattice and the electronic thermal conductivities. Figure 3(b) also shows that, when the lateral momentum of electrons is not conserved, the electronic thermal conductivity should have a strong dependence on the doping concentration with the range being 1.2 W/m K. This is a significant fraction of the measured total thermal conductivity of 2.8 ± 0.5 W/m K. On the other hand, the lateral momentum of electrons is conserved, the electronic thermal conductivity shows marginal dependence on doping concentration with the range being 0.4 W/m K, which is within the experimental uncertainty. It should be noted that the lattice thermal conductivity should be almost

independent of doping concentration. Hence, the measurements suggest that the electronic thermal conductivity should have at most marginal dependence on doping concentration with the range being 0.5 W/m K. Therefore, one can conclude that the actual electronic thermal conductivity should be close to that based on the assumption of lateral momentum conservation of electron momentum. In fact, previous transient ZT measurements on the same materials support this conclusion.¹⁹ This suggests that there is lateral conservation of electronic momentum during thermionic emission in the superlattices, which limit the fraction of available electrons for thermionic emission, thereby affecting performance of thermoelectric devices.¹⁷

In summary, the total cross-plane thermal conductivity of ErAs:InGaAs/InGaAlAs superlattices is almost identical even though doping levels of the four samples are different. Also, the lattice thermal conductivity should be almost independent of doping. Therefore, the electronic thermal conductivity should have marginal dependence on doping concentration. Based on these arguments and theoretical analysis, it was deduced that the actual electronic thermal conductivity should be close to those based on the assumption that lateral momentum during thermionic emission is conserved, which limit the fraction of available electrons for thermionic emission.

This work was supported by the Office of Naval Research (ONR) Multidisciplinary University Research Initiative (MURI) Grant with Dr. Mihal E. Gross as a project manager.

¹R. Venkatasubramanian, Phys. Rev. B **61**, 3091 (2000).

²R. Venkatasubramanian, E. Siivola, T. Colpitts, and B. O'Quinn, Nature (London) **413**, 597 (2001).

³T. C. Harman, P. J. Taylor, M. P. Walsh, and B. E. LaForge, Science **297**, 2229 (2002).

⁴T. Borca-Tasciuc, W. L. Liu, J. L. Liu, T. F. Zeng, D. W. Song, C. D. Moore, G. Chen, K. L. Wang, M. S. Goorsky, T. Radetic, R. Gronsky, T. Koga, and M. S. Dresselhaus, Superlattices Microstruct. **28**, 199 (2000).

⁵J. C. Caylor, K. Coonley, J. Stuart, T. Colpitts, and R. Venkatasubramanian, Appl. Phys. Lett. **87**, 023105 (2005).

⁶J. M. Zide, D. O. Klenov, S. Stemmer, A. Gossard, G. H. Zeng, J. E. Bowers, D. Vashaee, and A. Shakouri, Appl. Phys. Lett. **87**, 112102 (2005).

⁷D. G. Cahill, Rev. Sci. Instrum. **61**, 802 (1990).

⁸W. Kim, J. M. Zide, A. Gossard, D. Klenov, S. Stemmer, A. Shakouri, and A. Majumdar, Phys. Rev. Lett. **96**, 045901 (2006).

⁹J. M. Ziman, Philos. Mag. **1**, 191 (1956).

¹⁰C. L. Tien, A. Majumdar, and F. M. Gerner, *Microscale Energy Transport* (Taylor & Francis, Washington, DC, 1998).

¹¹J. F. Bresse and A. C. Papadopoulos, J. Appl. Phys. **64**, 98 (1988).

¹²J. R. Drabble and H. J. Goldsmid, *Thermal Conduction in Semiconductors* (Pergamon, Oxford, NY, 1961).

¹³G. S. Kumar, G. Prasad, and R. O. Pohl, J. Mater. Sci. **28**, 4261 (1993).

¹⁴Sadao Adachi, *Physical Properties of III-V Semiconductor Compounds: InP, InAs, GaAs, GaP, InGaAs, and InGaAsP* (Wiley, New York, 1992).

¹⁵D. Vashaee and A. Shakouri, J. Appl. Phys. **95**, 1233 (2004).

¹⁶D. L. Smith, E. Y. Lee, and V. Narayanamurti, Phys. Rev. Lett. **80**, 2433 (1998).

¹⁷D. Vashaee and A. Shakouri, Phys. Rev. Lett. **92**, 106103 (2004).

¹⁸H. Ehrenreich, J. Appl. Phys. **32**, 2155 (1961).

¹⁹R. Singh, Z. Zhixi Bian, D. Vashaee, A. Shakouri, J. M. O. Zide, G. Zeng, H. Chou, A. Gossard, and J. Bowers, Mater. Res. Soc. Symp. Proc. **886**, 0886-F04-04.1 (2006).